HHS Public Access

Author manuscript

Hepatology. Author manuscript; available in PMC 2017 March 01.

Published in final edited form as:

Hepatology. 2016 March ; 63(3): 965–982. doi:10.1002/hep.28382.

MACROPHAGE RECRUITMENT BY FIBROCYSTIN-DEFECTIVE BILIARY EPITHELIAL CELLS PROMOTES PORTAL FIBROSIS IN CONGENITAL HEPATIC FIBROSIS

Luigi Locatelli[1,†], **Massimiliano Cadamuro**[1,2,†], **Carlo Spirli**[3], **Romina Fiorotto**[3], **Silvia Lecchi**[4], **Carola Maria Morell**[1], **Yury Popov**[5], **Roberto Scirpo**[1], **Maria De Matteis**[2], **Mariangela Amenduni**[3], **Andrea Pietrobattista**[6], **Giuliano Torre**[6], **Detlef Schuppan**[5,7], **Luca Fabris**[2,3,*], and **Mario Strazzabosco**[1,3]

[1]Department of Surgery and Translational Medicine, University of Milan-Bicocca, 20126, Milan, Italy

[2]Department of Molecular Medicine, University of Padua School of Medicine, 35121, Padua, Italy

[3]Section of Digestive Diseases, Yale University, New Haven, CT 06520, USA

[4]Center for Liver Research (CeLiveR), Papa Giovanni XXIII Hospital, 24121, Bergamo, Italy

[5]Division of Gastroenterology, Beth Israel Deaconess Medical Center, Harvard Medical School, Boston, MA 02215, USA

[6]Liver Unit, Bambino Gesu Pediatric Hospital, IRCSS, 00146, Rome, Italy

[7]Institute of Translational Immunology, Johannes Gutenberg University, 55122, Mainz, Germany

Abstract

Congenital Hepatic Fibrosis (CHF) is a disease of the biliary epithelium characterized by bile duct changes resembling ductal plate malformations and by progressive peribiliary fibrosis, in the absence of overt necroinflammation. Progressive liver fibrosis leads to portal hypertension and liver failure, however the mechanisms leading to fibrosis in CHF remain elusive. CHF is caused by mutations in *PKHD1*, a gene encoding for fibrocystin, a ciliary protein expressed in cholangiocytes. Using a fibrocystin-defective (*Pkhd1*$^{del4/del4}$) mouse, which is orthologous of CHF, we show that *Pkhd1*$^{del4/del4}$ cholangiocytes are characterized by a β-catenin-dependent secretion of a range of chemokines, including CXCL1, CXCL10 and CXCL12, which stimulate bone marrow-derived macrophage recruitment. We also show that *Pkhd1*$^{del4/del4}$ cholangiocytes, in turn, respond to proinflammatory cytokines released by macrophages by up-regulating αvβ6 integrin, an activator of latent local TGFβ1. While the macrophage infiltrate is initially dominated by the M1 phenotype, the profibrogenic M2 phenotype increases with disease progression, along with the number of portal myofibroblasts. Consistent with these findings, clodronate-induced

[*]**Correspondence**. Luca Fabris M.D., Ph.D., Department of Molecular Medicine, University of Padova School of Medicine, Viale G. Colombo, 3; 35131 Padova, Italy, Phone: +39 049 827 6127; Fax: +39 049 807 3310, luca.fabris@unipd.it; luca.fabris@yale.edu.
[†]These authors contributed equally to this work

DISCLOSURE

All authors have no conflict of interest regarding this study to declare.

macrophage depletion results in a significant reduction of portal fibrosis and portal hypertension as well as of liver cysts.

Conclusion—our results show that fibrosis can be initiated by an epithelial cell dysfunction, leading to low-grade inflammation, macrophage recruitment and collagen deposition. These findings establish a new paradigm for biliary fibrosis and represent a model to understand the relationship between cell dysfunction, parainflammation, liver fibrosis and macrophage polarization over time.

Keywords

congenital hepatic fibrosis; fibrocystin; transforming growth factor (TGF)-β1; tumor necrosis factor (TNF)-α; biliary cyst

Untreated chronic liver diseases lead to cirrhosis, portal hypertension, and clinical decompensation. The main mechanism of disease progression is liver fibrosis, i.e. the deposition of collagen in the portal space and/or around the hepatocytes, which is responsible for architectural distortion and vascular changes. Liver fibrosis is usually the result of an ongoing reparative response to an unresolving necroinflammatory damage to the liver epithelia. However, some liver conditions, such as hepatoportal sclerosis and congenital hepatic fibrosis, do not follow this paradigm, and fibrosis appears to be rather caused by a non-classical inflammatory process in the portal space without necrotic damage.

Congenital hepatic fibrosis (CHF) is a genetic cholangiopathy caused by mutations in *PKHD1*, the gene encoding for fibrocystin/polyductin (FPC), a protein of unknown function expressed on cilia and centromers of bile duct and renal tubular epithelial cells[1,2]. In the liver, FPC deficiency leads to the formation of biliary microhamartomas and segmental dilations of bile ducts accompanied by progressive portal fibrosis, resulting in clinically relevant portal hypertension[3]. Complications of portal hypertension are a major cause of morbidity and mortality in CHF[4]. It is expected that the ability to reduce the progression of fibrosis in CHF would improve survival. Unfortunately, the mechanisms responsible for portal fibrosis in CHF are unknown.

Recent studies have identified several defects of intracellular signaling in FPC-deficient cells, including increased cAMP/PKA signaling[5] and PKA-dependent β-catenin activation[5]. β-catenin is emerging as a novel regulator of inflammation, able to influence cytokine secretion in experimental liver cancer[6]. It has been proposed that a persistent, not resolving cell dysfunction may promote a chronic, low-grade inflammatory response (defined by Medzhitov as “parainflammation”) that can ultimately lead to scarring[7]. Interestingly, an increased production of pro-inflammatory cytokines has been reported in fibropolycystic liver diseases[8,9].

In this study, we have used a mouse orthologous of human CHF that harbours a homozygous deletion in exon4 of the *Pkhd1* gene[10] to investigate the pathogenesis of liver fibrosis in CHF. Our data provide strong evidence that fibrosis is the result of a low-level chronic inflammatory response generated by FPC-defective cholangiocytes that secrete chemokines able to recruit bone marrow-derived macrophages and, in turn, respond to

cytokines released by macrophages by up-regulating the αvβ6 integrin, a local TGFβ1 activator. In contrast with other experimental models of liver fibrosis, collagen deposition in *Pkhd1*$^{del4/del4}$ mice initiates with little contribution from myofibroblasts, but then accelerates as the proportion of M2 polarized macrophages, TGFβ1 production and portal myofibroblasts increase. In line with these data, macrophage depletion with clodronate, reduces αvβ6 integrin biliary expression and myofibroblast accumulation and halts fibrosis progression and the development of portal hypertension, in conjunction with a significant reduction in liver cysts. Our results provide a new paradigm for biliary fibrosis and represent a model to understand the relationship between cell dysfunction, parainflammation, liver fibrosis and macrophage polarization over time.

MATERIALS AND METHODS

Animal model

We used the Pkhd1$^{del4/del4}$ mouse (a kind gift from S. Somlo, Yale University, New Haven, CT), an accepted model for the human CHF disease[10]. All animals were housed at the Yale Animal Care facility and received human care according to the Yale IACUC protocols. See supplemental materials for mouse model details.

Assessment of portal fibrosis by Sirius Red staining

Sirius red histochemistry was performed to assess the extension of portal fibrosis and its progression through maturation. Liver sections were obtained from *Pkhd1*$^{del4/del4}$ and WT mice at different maturation ages. See supplemental material for details.

Portal hypertension was assessed by measuring the spleen weight

in the same mice analyzed for portal fibrosis. For each animal, the spleen weight was normalized to the respective body weight, and used as measure of portal hypertension[11].

In vivo clodronate treatment

To induce a selective macrophage depletion, *Pkhd1*$^{del4/del4}$ mice of 3 months of age were treated for 3 months with clodronate liposomes (100mg/kg every three days, I.P., n=4) or with vehicle (sterile phosphate-buffered saline (PBS) + liposomes every three days by I.P., n=3)[12]. At the end of treatment, mice were sacrificed to assess the extent of peribiliary fibrosis by Sirius Red, the cystic area by immunohistochemistry for K19, the number of α-SMA$^+$, F4/80$^+$ and CD45$^+$ cells in the portal area, the number of αvβ6 integrin$^+$ cysts and the spleen/body weight ratio.

Human tissues samples of CHF

Formalin-fixed, paraffin-embedded archival tissue specimens of CHF patients obtained from percutaneous needle liver biopsy (n=3) and surgical specimens from liver transplant explants (n=2) or liver resection (n=1) were considered for the immunohistochemical study. All specimens were reviewed to confirm the histopathological diagnosis of CHF. Patients undergoing liver transplantation or liver resection were complicated by portal hypertension,

which instead was absent in patients undergoing needle biopsy. Informed consent and local regional ethical committee approval were obtained before tissue collection.

Expression of αvβ6 integrin, Snail1, p-Smad3, and phenotypic characterization of the portal inflammatory cell infiltrate by immunohistochemistry in human and murine samples

Liver tissue sections obtained from both *Pkhd1*$^{del4/del4}$ mice and archived biopsies of CHF patients with different degree of portal fibrosis were considered to study the expression of αvβ6 integrin along with Snail1 and pSmad3, as signatures of TGFβ1 activation, and the phenotype of the portal cell infiltrate using the following markers: cytokeratin-19 (K19) (cholangiocyte), CD45 (leukocyte), NIMP-R14 (neutrophil), F4/80 (macrophage), MAC387 (bone marrow-derived macrophage), CD68 (resident macrophage), inducible nitric oxide synthase (iNOS, M1 macrophage), CD206 (M2 macrophage), collagen-I, α-smooth muscle actin (α-SMA) (myofibroblast), and elastin (ELN, portal myofibroblast). See supplemental material for details.

Quantification of K19$^+$, α-SMA$^+$, ELN$^+$, CD45$^+$, F4/80$^+$/iNOS$^+$ and F4/80$^+$/CD206$^+$ cells, and αvβ6 integrin expression

by immunohistochemistry is described in supplemental material.

Expression of β6 mRNA, fibrosis-related transcripts and cyto/chemokines by quantitative real-time RT-PCR

Total RNA was isolated from liver tissue as described[13], to measure the expression of β6 integrin, TGFβ1, TNFα, and Procollagen α1(I) (COL1(A1)), as previously reported[14]. See supplemental material for further details.

Liver non-parenchymal cell isolation and fluorescence-activated cell sorting (FACS) analysis

FACS analysis was performed to characterize the different cell subsets contributing to the portal inflammatory cell infiltrate. Liver non-parenchymal cells were isolated in the Cell Isolation Core of the Yale Liver Center. See supplemental material for details.

Isolation and characterization of cholangiocytes

Mouse cholangiocytes were isolated from *Pkhd1*$^{del4/del4}$ and WT mice at 3 months of age as previously described[5].

Macrophage recruitment by conditioned media from *Pkhd1*$^{del4/del4}$ cholangiocytes

To test the polarity-dependent ability of *Pkhd1*$^{del4/del4}$ cholangiocytes to recruit macrophages, we studied the effect of conditioned medium differentially harvested from basolateral and apical sides, on a mouse macrophage cell line (RAW264.7). Further information are detailed in the supplemental section.

Assessment of macrophage migration induced by CXCL1 and CXCL10

To evaluate whether cytokines significantly secreted by *Pkhd1*$^{del4/del4}$ cholangiocytes in the basolateral medium (CXCL1, CXCL10) could represent homing signals for inflammatory

cells, we studied their ability to stimulate cell migration in macrophages, using murine RAW 264.7 macrophages. The mouse recombinant proteins CXCL1 and CXCL10 (PeproTech, London, UK) were tested at the dose of 1ng/ml in Boyden chambers.

Determination of cytokine secretion in *Pkhd1*$^{del4/del4}$ cholangiocytes

In supernatant from the basolateral and apical sides of polarized cholangiocyte monolayer, a panel of 32 mouse chemokines and cytokines (see Suppl. Table 1) was analyzed using the Millipore's MILLIPLEX™ mouse Cytokines/Chemokines kit coupled with the BioPlex Luminex platform. See supplementary material for details.

Assessment of macrophage production of TGFβ1 and TNFα induced by CXCL1 and CXCL10

To evaluate whether CXCL1, CXCL10 and CXCL12 were also able to induce cytokine secretion by inflammatory cells, we studied their ability to stimulate expression of TGFβ1 and TNFα transcripts in RAW 264.7 cells. Cultured macrophages were tested with the mouse recombinant proteins CXCL1, CXCL10 (PeproTech, London, UK) at 1ng/ml and CXCL12 (R&D Systems, Milan, Italy) at 100 μg/ml, for 12h. Further details are given in supplemental material section.

Effects of TGFβ1 and TNFα on β6 mRNA expression on cultured cholangiocytes before and after the inhibition of the TGFβ receptor type II

To ascertain if TNFα stimulated separate signaling pathways to directly modulate the β6 expression, independently from a TGFβ1 loop, experiments of cytokine stimulation were run before and after preincubation for 24h of cultured cholangiocytes with a dominant negative, recombinant soluble TGFβ receptor type II-Fc fusion protein (rsTGF-βRII-Fc)(10ng/ml) (kind gift of Stromedix/Biogen, Inc., USA). rsTGF-βRII-FC is a chimeric construct inhibiting TGFβ1 signaling, in which the extracellular portion of TGFβRII was fused to an immunoglobulin heavy chain Fc fragment. By blocking specifically TGFβRII, this antibody prevents the association of TGFβRII with TGFβRI and therefore, its phosphorylation. See supplementary material for details.

Effects of TGFβ1 on COL1(A1) and Snail1 mRNA expression by cultured cholangiocytes

After starvation for 24h, polarized cultured primary cholangiocytes were treated for 24h with the recombinant murine TGFβ1 (1ng/ml). Before and after TGFβ1 stimulation, COL1(A1), and Snail1 mRNA expression was determined in total RNA from cultured cells (see above).

Statistical Analysis

is detailed in the supplemental section.

RESULTS

Pkhd1$^{del4/del4}$ mice as disease model for CHF

Pkhd1$^{del4/del4}$ mice bear an inactivating deletion in the exon 4 of the *Pkhd1* gene[10]. Serial analysis of *Pkhd1*$^{del4/del4}$ mouse liver and spleen demonstrate an age-dependent increase in the biliary cystic malformations (Supplemental Fig.1A–B), peribiliary fibrosis (Fig.1A), increased collagen-I deposition, as shown by the progressive increase in Sirius Red staining (Fig.1B) and in COL1(A1) (procollagen α1(I)) gene expression, as compared to wild type (WT) littermates (Fig.1C). Deposition of fibrosis begins in the pericystic region, and then extended through the portal area, finally leading to portoportal septa formation (Fig.1A). Significant splenomegaly, indicative of clinical portal hypertension, becomes evident between 6 and 9 months after birth, and increases further up to 12 months of age (Fig.1D); splenomegaly strongly correlates with Sirius Red staining ($r=0.96$, $p<0.01$)(Fig.1E). The histological biliary lesions and the slow progression of fibrosis, leading to portal hypertension, are consistent with the morphology and the natural history of human CHF, and establish the *Pkhd1*$^{del4/del4}$ mice as a reliable disease model.

Early peribiliary infiltration with CD45$^+$ cells, mostly macrophages

Development of pericystic fibrosis was associated with the progressive accumulation of inflammatory cells in the portal tracts, which localized in close vicinity to the biliary cysts, as observed by immunohistochemistry for CD45$^+$ (Fig.2A). By 9 months of age the percentage of the portal tract area infiltrated by CD45$^+$ cells increased up to 25% (Fig.2B). In contrast, the number of myofibroblasts (α-SMA$^+$ cells) was initially limited (Fig.2C–D); these cells were positive for the portal fibroblast biomarker ELN, and their number similarly increased progressively (Fig.2E–F). Phenotypic characterization of the inflammatory cell infiltrate by FACS analysis (CD45$^+$-based cell selection), and by combined immunohistology for CD45 and F4/80 (macrophage marker) or NIMP-R14 (neutrophil marker), showed that the majority of the infiltrating CD45$^+$ cells were macrophages, based on their co-expression of CD11b and F4/80 (Supplemental Fig.2A). The percentage of CD45$^+$/CD11b$^+$/F4/80$^+$ cells ranged from 57 to 68% of the total CD45$^+$ cell population without significant changes over time. The contribution of neutrophils (CD45$^+$/Ly6G$^+$) and monocytes (CD45$^+$/CD11b$^+$/Ly6G$^-$/F4/80$^-$) was consistently much lower than that of macrophages (Supplemental Fig.2B). Immunohistochemistry showed that the majority of CD45$^+$ cells were F4/80$^+$ and were localized in the portal space along the profile of the cysts (Supplemental Fig.2C and Supplemental Fig.2E). In contrast with F4/80 cells, NIMPR14$^+$ cells contributed minimally to the CD45$^+$ cell population, being limited to small cell clumps (Supplemental Fig.2D). By dual immunofluorescence for CD68 (marker of local resident macrophages) and MAC387 (marker of bone marrow-derived macrophages) combined with the biliary marker K19, we found that peribiliary macrophages predominantly expressed MAC387, while the amount of CD68$^+$ cells infiltrating the portal area was negligible until 9 months (Supplemental Fig.3A,B). Microbiological analysis showed that *Pkhd1*$^{del4/del4}$ livers from all ages were sterile (not shown); in addition, gut decontamination with polymyxin B and neomycin had no effect on the progressive accumulation of CD45$^+$ cells in the portal space (not shown). Preponderance of CD45$^+$ inflammatory cells on α-SMA$^+$ myofibroblasts and ELN$^+$ portal fibroblasts in the peribiliary infiltrate was confirmed in liver biopsies from

CHF patients at a stage not yet complicated by portal hypertension (Supplemental Fig.4A); α-SMA$^+$ myofibroblasts and ELN$^+$ portal myofibroblasts became prevalent in more advanced disease undergoing liver transplantation because of complications of portal hypertension (Supplemental Fig.4B).

Changes in macrophage polarization over time

Among F4/80$^+$ cells, the subset co-expressing iNOS (M1 polarization marker) was preponderant over that co-expressing CD206 (M2 marker). However the relative contribution of M2 macrophages increased progressively, matching that of M1 at 12 months (Fig.3A–C). Consistent with this observation, hepatic gene expression of TGFβ1 (an M2 cytokine) was only modestly increased in the early phases, becoming significant at 9 months (2.5-folds as respect to WT) (Fig.3D), whereas TNFα (an M1 cytokine) mRNA was strongly up-regulated since the early stage of the disease, reaching 80-fold expression with respect to WT at 9 months (Fig.3E).

Expression of αvβ6 integrin, an activator of latent TGFβ1, is up-regulated in the cystic epithelium of *Pkhd1*$^{del4/del4}$ mice in response to the macrophage-derived cytokines TGFβ1 and TNFα

The αvβ6 integrin, an activator of latent TGFβ1 that is expressed by reactive cholangiocytes during liver repair, increased progressively between 1 and 12 months (Fig.4A–B). Expression of αvβ6 integrin was restricted to biliary cysts, and was negative in bile ducts of WT littermates. The immunohistochemical expression of αvβ6 integrin on cystic epithelia strongly correlated with portal fibrosis as measured by Sirius red ($r=0.94$, $p<0.02$) (Fig.4C). Notably, αvβ6 integrin was expressed in cysts surrounded by a dense macrophage infiltrate (Fig.4E) and the number of αvβ6 integrin$^+$ cysts correlated with the extent of CD45$^+$ cell infiltration ($r=0.97$, $p<0.01$) (Fig.4D), thereby suggesting a relationship between peribiliary recruitment of inflammatory cells and αvβ6 up-regulation in biliary cysts. Thus, we studied whether the macrophage-derived cytokines TNFα and TGFβ1 were able to regulate the expression of β6 (the rate limiting subunit for the formation of the αvβ6 integrin dimer) mRNA in cultured *Pkhd1*$^{del4/del4}$ cholangiocytes. We found that β6 mRNA, already significantly increased in basal conditions in *Pkhd1*$^{del4/del4}$ cholangiocytes as compared with WT, was further and significantly increased by stimulation with either TNFα or TGFβ1 ($p<0.05$). Blockade of the TGFβRII receptor abolished the effects of TGFβ1 on β6 gene expression, but not those of TNFα (Fig.4F), indicating that TNFα effects are TGFβ1-independent. Interestingly, the stimulatory effect of TNFα on β6 was observed only in *Pkhd1*$^{del4/del4}$ cholangiocytes that already have increased expression levels of β6, an observation again consistent with a pro-inflammatory phenotype of cystic cells in FPC-deficiency. The ability of TNFα to up-regulate αvβ6, thereby activating latent TGFβ1, is likely involved in peribiliary collagen deposition in the early phases of the disease, when TGFβ1 expression is only mildly up-regulated and M1 macrophages predominate. Immunohistochemical analysis of serial liver sections from *Pkhd1*$^{del4/del4}$ mice and from archival specimens of CHF patients showed nuclear expression of Snail1 and pSmad3 (transcription factors activated by TGFβ1 signaling) in cystic cells expressing αvβ6 (Supplemental Fig.5). This findings provides clear evidence that TGFβ1 signaling is locally

activated in αvβ6-expressing cysts, and that the findings described in *Pkhd1*$^{del4/del4}$ mice are actually relevant also for patients with CHF.

Factors secreted by *Pkhd1*$^{del4/del4}$ cholangiocytes recruit macrophages at their basolateral pole

Having shown that in the early phases of the disease, the pericystic spaces of *Pkhd1*$^{del4/del4}$ mice are infiltrated more by macrophages than by myofibroblasts, and that cytokines characteristic either of the M1 or M2 polarization are able to up-regulate αvβ6 integrin, thereby promoting a pericystic fibrogenic response, we hypothesized that macrophages could be attracted into the pericystic area by soluble factors secreted by the *Pkhd1*$^{del4/del4}$ cholangiocytes themselves. Therefore, we studied the transwell migration of the macrophage cell line RAW 264.7, after exposure to conditioned media collected from the apical or basolateral sides of polarized monolayers of WT or *Pkhd1*$^{del4/del4}$ cholangiocytes (isolated from 3 months old mice). Macrophage migration was significantly higher after exposure to conditioned media from *Pkhd1*$^{del4/del4}$ than from WT cholangiocytes; furthermore, the basolateral medium from *Pkhd1*$^{del4/del4}$ cholangiocytes significantly stimulated macrophage recruitment, and did so more strongly than the apical medium. Interestingly, recruitment of RAW 264.7 macrophages was significantly lower when challenged with conditioned medium from cells exposed to β-catenin inhibitors such as quercetin or ICG-001 (Fig.6A). Collectively, these data are consistent with the hypothesis that *Pkhd1*$^{del4/del4}$ cholangiocytes secrete paracrine factors able to recruit macrophages through a β-catenin-dependent mechanism.

To identify the factors possibly involved in macrophage recruitment by *Pkhd1*$^{del4/del4}$ cholangiocytes, we first measured the gene expression of a number of cytokines previously shown to be secreted by cholangiocytes in culture. As shown in Fig.5, we used laser capture microdissection (LCM) of the epithelial cysts in *Pkhd1*$^{del4/del4}$ vs bile ducts in WT littermates at 1 and 3 months of age. We found that increased gene expression of SDF-1/CXCL12 and LIX/CXCL5 represented the earliest changes in cystic structures of *Pkhd1*$^{del4/del4}$ mice (Fig.5A) followed at 3 months by KC/CXCL1, IP-10/CXCL10, MIP-2/CXCL2 and IL-1β (Fig.5B). All these cytokines possess chemotactic functions for monocytes and macrophages. To verify that the above cytokines were actually secreted by *Pkhd1*$^{del4/del4}$ cholangiocytes, we measured their secretion at the basolateral medium of cultured cholangiocyte monolayers. Supplemental Table 1 shows the cyto/chemokines secreted into the basolateral medium by *Pkhd1*$^{del4/del4}$ cholangiocytes. Among them, some such as CXCL1, CXCL10 and CXCL12, were significantly more secreted by cultured *Pkhd1*$^{del4/del4}$ cells, others, including MCP-1/CCL2 and CXCL5, showed a clear trend towards an increased secretion in *Pkhd1*$^{del4/del4}$ cholangiocytes with respect to WT.

CXCL12 is a well-known chemoattractant for macrophages[15]; less is known about CXCL1 and CXCL10. By exposing macrophages to the relative recombinant chemokines, we found that both CXCL1 and CXCL10 were able to significantly stimulate transwell migration of RAW 264.7 cells (Supplemental Fig.6A) (either 1ng/ml). Furthermore, CXCL1 and CXCL10 but not CXCL12 were able to up-regulate the expression of TGFβ1 and TNFα transcript in macrophages (Supplemental Fig.6B–C). The pathogenetic relevance of the

chemotactic effect of CXCL1, CXCL10 and CXCL12 on macrophage was confirmed by the significant reduction of macrophage migration after administration of their specific blocking antibodies or inhibitors to the basolateral conditioned medium of *Pkhd1*$^{del4/del4}$ cholangiocytes. Notably, the combined administration of the three specific blockers to the basolateral medium of the *Pkhd1*$^{del4/del4}$ cholangiocytes had a synergic effect in reducing the macrophage transwell migration reaching an extent comparable to the one measured after administration of the β-catenin inhibitors, without any effect on cell viability (Fig.6A). In *Pkhd1*$^{del4/del4}$ cholangiocytes exposed to β-catenin inhibitors (quercetin or ICG-001), gene expression and protein secretion of CXCL1, CXCL10 and CXCL12 were significantly inhibited (Fig.6B–D). This finding establishes a mechanistic relationship between the increased production of CXCL1, CXCL10 and CXCL12 and a known signaling defect of *Pkhd1*$^{del4/del4}$ cholangiocytes.

Gene expression of COL1(A1) and Snail1 is increased in *Pkhd1*$^{del4/del4}$ cells and is further stimulated by TGFβ1

Because the biological activity of TGFβ1 is enhanced in the vicinity of cells displaying αvβ6 integrin, we studied the effects of TGFβ1 on COL1(A1) mRNA expression in cultured cholangiocytes, a cell type which is not commonly considered as a source of procollagen-I. As compared to WT, *Pkhd1*$^{del4/del4}$ cholangiocytes showed increased basal levels of COL1(A1) mRNA ($p<0.01$), which were further up-regulated by TGFβ1 (1ng/ml)($p<0.05$). This was not observed in WT cholangiocytes (Supplemental Fig.7A). Similarly, Snail1 mRNA basal levels were higher in *Pkhd1*$^{del4/del4}$ cholangiocytes, and were further stimulated by TGFβ1 (Supplemental Fig.7B). Again, increased gene expression of COL1(A1) was confirmed in biliary cysts analyzed after isolation via LCM at 1 and 3 months (Supplemental Fig.7C). These data are consistent with the observation that TGFβ1 signaling is functionally active in FPC-defective cholangiocytes (Supplemental Fig.5) and that collagen-I, stimulated by locally activated TGFβ1, starts to be deposited in close vicinity to biliary cysts, when myofibroblasts are scarce or absent (Supplemental Fig.7D).

Macrophage depletion by clodronate in *Pkhd1*$^{del4/del4}$ mice treated from 3 to 6 months, halts fibrosis progression and development of portal hypertension, and reduces αvβ6 integrin biliary expression, macrophage infiltration, myofibroblast activation and biliary cyst area

To confirm the pathogenetic role of macrophages in regulating biliary fibrogenesis in FPC deficiency, we tested the effects of macrophage depletion following a 3-month treatment with clodronate (Supplemental Fig.8A–B). We chose the interval from 3 through 6 months as critical window of fibrogenesis preceding the development of portal hypertension. At the end of treatment, the number of macrophages infiltrating the portal space was comparable to that of the starting time, being reduced by about 60% with respect to paired controls (Fig. 7A–B and Supplemental Fig.9A), without significant changes in the proportion between M1 and M2. Interestingly, macrophage depletion was associated with a significant decrease in the expression levels of αvβ6 on biliary structures (Fig.7D and Supplemental Fig.9C) and in myofibroblast accumulation in the portal space (Fig.7C and Supplemental Fig.9B). These effects were accompanied by a striking reduction in Sirius Red staining of the peribiliary area (Fig.7E and Supplemental Fig.9D) together with a significant decrease in biliary cysts

(Supplemental Fig.8C–E). Noteworthy, reducing peribiliary fibrosis at this stage is clinically relevant since it prevents development of portal hypertension, as shown by the absence of significant splenomegaly in treated mice (Fig. 7F).

DISCUSSION

Portal fibrosis is the main mechanism of chronic liver disease progression. Most experimental studies on liver fibrosis use models of obstructive cholestasis or toxin-induced necroinflammatory biliary or parenchymal damage. However, genetic diseases offer unique opportunities to probe fundamental disease mechanisms. In this study, we investigated the mechanisms of liver fibrosis in CHF, a genetic fibropolycystic liver disorder, characterized by progressive peribiliary fibrosis and portal hypertension.

We show that in CHF, fibrosis develops in two phases. During the slowly progressing preclinical phase, bone marrow-derived macrophages are recruited by chemokines secreted by the FPC-defective cystic epithelium. TNFα, secreted by classically activated M1-macrophages, up-regulates epithelial expression of αvβ6 integrin (an effect specific of FPC-defective cholangiocytes) that then activates latent TGFβ1 in the vicinity of the cystic epithelium. We have also found that cholangiocytes respond to TGFβ by producing procollagen α1(I). While this may actually promote peribiliary fibrosis during the early phases of the disease, further studies are needed to unequivocally demonstrate the ability of these cells to produce collagen. In the early phase, infiltrating myofibroblasts are scarce, but their number, essentially represented by portal fibroblasts, increases during the second phase of accelerating fibrogenesis, as the proportion of alternatively activated M2 macrophages increases along with the expression of TGFβ1 and collagen-I, and portal hypertension becomes clinically evident. Thus in CHF, a genetically determined dysfunction of epithelial cell homeostasis promotes the secretion of chemokines able to recruit macrophages that orchestrate a pro-fibrotic tissue response switching from an inflammatory to a reparative phenotype.

For these studies, we used an animal model (*Pkhd1*$^{del4/del4}$ mouse) that reproduces the clinical and histological features of human CHF. This model presents unique features, as compared to other experimental models of portal fibrosis, such as bile duct ligation (BDL), or sclerosing cholangitis caused by Mdr2-deficiency[14,16] or toxicants. In fact, in *Pkhd1*$^{del4/del4}$ mice, fibrosis is not related to a necroinflammatory or obstructive process and the evolution of biliary fibrosis is slow: it resembles that of human CHF, in which portal hypertension occurs in the absence of cirrhosis and is generally diagnosed only late in youth[17].

In contrast with Mdr2-KO mice[13] and BDL, in which there is an early and a massive increase in periportal α-SMA$^+$ myofibroblasts, in *Pkhd1*$^{del4/del4}$ mice, in spite of increased procollagen α1(I) levels, a significant increase in α-SMA$^+$ cells, mainly related to ELN$^+$ portal myofibroblast[18,19] accumulation, is detected only later, once portal fibrosis is already established. Our data show an early and progressive accumulation of mononuclear CD45$^+$ inflammatory infiltrate in the portal space (mostly macrophages) suggesting that the defect in epithelial cell FPC expression causes a chronic, low-grade inflammatory process and

initial collagen deposition. Our findings also indicate that recruited macrophages are likely of bone marrow origin (based on their expression of MAC387)[20], while the contribution of endogenous, yolk sac-derived macrophages ($CD68^+$) is negligible[21]. Studies in archival human CHF specimens, confirmed an early portal infiltration with $CD45^+$ cells in absence of α-SMA^+ and ELN^+ cells in early cases without portal hypertension, thus indicating that our findings have translational relevance.

This low-grade chronic inflammation (defined by Medzhitov as "parainflammation") is a process of adaptation to an unresolving cell dysfunction or noxious condition[7]. When the cell dysfunction is persistent, the inflammatory response, unable to restore the normal tissue homeostasis, becomes pathologic and stimulates the deposition of scar tissue[22]. Consistent with prior reports showing increased cytokine and growth factor production in fibropolycystic liver diseases[8,9], our study demonstrates that FPC-defective cholangiocytes produce several chemokines. *In vivo* analysis of transcripts expressed in biliary cysts isolated by LCM from 1 and 3 months old *Pkhd1*$^{del4/del4}$ shows that expression of specific chemokines (SDF-1/CXCL12, LIX/CXCL5, KC/CXCL1, IP-10/CXCL10, MIP-2/CXCL2, IL-1β) is increased since the early stages of the disease. Furthermore, we found that the medium of polarized *Pkhd1*$^{del4/del4}$ cholangiocytes is able to recruit macrophages much more intensely than medium from WT cholangiocytes. Recruiting effect of the basolateral medium was much stronger than the apical medium, indicating that chemokine secretion is polarized. Measuring the basolateral concentration of a panel of cyto/chemokines, we confirmed that *Pkhd1*$^{del4/del4}$ cholangiocytes produce increased levels of soluble factors able to recruit macrophages, including MCP-1, CXCL1, CXCL5, CXCL10 and CXCL12. Among the above chemokines, the role of MCP-1 in biliary pathophysiology has been extensively studied; cholangiocytes can secrete MCP-1 in culture[23], and *in vivo*, following liver damage induced by BDL or hydrophobic bile acid intoxication, MCP-1 secretion increases together with the extent of portal inflammatory infiltrate[24,25].

Several signaling defects have been described in FPC-defective cells, including increased cAMP/PKA-mediated Ser^{675}-phosphorylation of β-catenin, leading to enhanced β-catenin transcriptional activity[5]. Recent findings indicate that β-catenin can act as a regulator of inflammation[5]. Consistent with this hypothesis, our data show that in *Pkhd1*$^{del4/del4}$ cholangiocytes, gene expression and secretion of CXCL1, CXCL10 and CXCL12 were inhibited by two different inhibitors of β-catenin transcriptional activity (quercetin and ICG-001)[5], suggesting that in FPC-deficiency, activation of β-catenin signaling promotes a persistent pro-inflammatory response that recruits macrophages near the biliary cysts. Notably, exposure to basolateral medium from β-catenin-inhibited *Pkhd1*$^{del4/del4}$ cholangiocytes was able to suppress macrophage recruitment to an extent similar to that obtained with the simultaneous antagonism of CXCL1, CXCL10 and CXCL12.

Whole liver expression of TNFα and TGFβ1 increased significantly in *Pkhd1*$^{del4/del4}$ mice and their expression in macrophages was stimulated by CXCL1 and CXCL10. Noteworthy, both TNFα and TGFβ1 increased $\alpha v\beta 6$ integrin expression on cholangiocytes, but inducing effects by TNFα were observed only in *Pkhd1*$^{del4/del4}$ cholangiocytes and were independent from TGFβ1 activation. Expression of $\alpha v\beta 6$ integrin was typically restricted to the cystic epithelium, where it was progressively up-regulated over time, and strongly correlated with

portal fibrosis. Furthermore, αvβ6 expression was accompanied by signatures of TGFβ1 activation in cholangiocytes (Snail1 and pSmad3 nuclear expression), also in human CHF specimens. TGFβ1 is in fact produced as an inactive latent precursor that is locally activated by αvβ6 integrin that cleaves the latency associated peptide[26].

TNFα and TGFβ1 are expressed by macrophages with pro-inflammatory (M1) and profibrotic (M2) functions, respectively[27]. During the natural course of a wound-healing response, classically-activated macrophages recruited to the site of damage first show a pro-inflammatory phenotype, with abundant secretion of TNFα. Then, to counteract the tissue-damaging potential of the inflammatory response, macrophages switch to an anti-inflammatory phenotype. If tissue damage persists, macrophages turns into a pro-fibrotic phenotype, whereby TGFβ1 expression is prevalent[28]. Our model is paradigmatic of this sequence, with an initial higher M1 proportion and a progressively increasing M2 contribution, matching that of M1 by 9 months, consistent with the observed time-dependent changes in TNFα and TGFβ1 expression. Interestingly, in addition to CXCL1 and CXCL10, CXCL5, which we found increased early in *Pkhd1*$^{del4/del4}$ biliary cysts *in vivo* by LCM, is also able to stimulate TNFα production in macrophages[29]. Given its early marked increase and its specific effects on epithelial αvβ6 expression on FPC-defective cholangiocytes, TNFα may contribute to local fibrogenesis in *Pkhd1*$^{del4/del4}$ mice, during the early phases of fibrosis, when most of TGFβ1 signaling is likely to derive from the activation of latent TGFβ1. Following activation by αvβ6, which occurs at the epithelial cell surface, TGFβ1 exerts its effects within the limits of the site of activation. The ability of reactive cholangiocytes to release fibrogenic growth factors, including PDGF-B[28], connective tissue growth factor[30], and extracellular matrix components, such as procollagen-IV[31] and laminin[32], is well known[26,27,30]. Our data show that in *Pkhd1*$^{del4/del4}$ cholangiocytes, procollagen-I transcripts are increased with respect to WT cholangiocytes both *in vitro* and *in vivo*, and are remarkably up-regulated by TGFβ1. *In vitro* susceptibility of *Pkhd1*$^{del4/del4}$ cholangiocytes to TGFβ1 effects was confirmed by the concomitant increased gene expression of the TGFβ1-dependent transcription factor Snail1. The concentration of TGFβ1 used for *in vitro* experiments (1ng/ml) is in the range of this cytokine found with tissue analysis. Higher TGFβ1 concentrations have an apoptotic effect on cholangiocytes in culture. Interestingly, in the same experimental model, we have recently shown that *Pkhd1*$^{del4/del4}$ cholangiocytes possess increased β-catenin-dependent migratory properties[5]. Increased migration and abnormal collagen deposition are consistent with the concept that FPC-defective epithelial cells are more prone to perform some limited mesenchymal functions. The direct involvement of cholangiocytes in driving collagen deposition, at least in the initial phase of fibrogenesis in *Pkhd1*$^{del4/del4}$ mice, may explain the distinctive features of this model, including the early peribiliary and slowly evolving matrix deposition. However, mesenchymal properties acquired by epithelial cells *in vitro*, should be interpreted with caution and further studies *in vivo* using mice reporter lines may help clarifying the question. After 6 months, when fibrosis accelerates and clinically relevant portal hypertension begins, ELN^{+} portal myofibroblasts becomes the relevant source of collagen.

The *in vivo* experiments with clodronate in *Pkhd1*$^{del4/del4}$ mice are consistent with this working model. By targeting macrophage infiltration at an age when portal hypertension is

not yet developed, we were able to show a stark reduction in macrophage infiltration, a decrease in the αvβ6 biliary expression and in the portal myofibroblast accumulation. These phenotypic alterations related to macrophage depletion are pathophysiologically relevant as they block progression of biliary fibrosis and prevent the development of portal hypertension. As a consequence of the reduction in macrophage infiltration, a reduction in the liver cyst area was noted, supporting the concept that macrophages exert a stimulatory effect on cyst growth.

In conclusion, we have shown that development of fibrosis in CHF follows a novel paradigm based on a complex interplay between epithelial, innate inflammatory and mesenchymal cells (Fig.8). These mechanisms suggest new, disease specific targets for antifibrotic therapies in CHF, a topic worth to be addressed in future studies.

Supplementary Material

Refer to Web version on PubMed Central for supplementary material.

ACKNOWLEDGMENTS

The authors wish to thank *Sheila Violette* (Stromedix Inc.) for kindly providing the TGFβRII blocking antibody, *Stephan Somlo*, Yale University, for the gift of *Pkhd1*$^{del4/del4}$ mice, and *Rafaz Hoque*, Yale University for the help with experiments with FACS analysis. *Alberto Mantovani*, University of Milan, *Ruslan Medzhitov*, Yale University, and *Maurizio Parola*, University of Turin, are gratefully acknowledged for critical revision of the manuscript and helpful comments. The authors are indebted to *Michele Colledan* and *Aurelio Sonzogni*, Papa Giovanni XXIII Hospital, Bergamo, and to *Paola Francalanci*, Bambino Gesu Pediatric Hospital, Rome, for providing histological samples of CHF patients, and to *Davide Viganò*, University of Sassari, for the help with Boyden chamber experiments.

Financial support.

Telethon (grant GGP09189) and Progetto di Ricerca Ateneo 2011 (grant CPD113799/11) to LF, LL and MC. NIH Grants DK079005 and DK034989 Silvio O. Conte Digestive Diseases Research Core Centers, projects CARIPLO 2011-0470 and PRIN 2009ARYX4T_005 to MS. “PSC partners seeking a cure” grant to MS and to RF. NIH grants 1R21A1 DK076873 and NIH U19 AI066313 to DS. NIH Grant RO1DK101528 to CS.

Abbreviations

ANIT	alpha-naphthylisothiocyanate
α-SMA	α-smooth muscle actin
BDL	bile duct ligation
bw	body weight
CD	cluster of differentiation
CHF	Congenital Hepatic Fibrosis
CXCL	Chemokine (C-X-C motif) ligand
DAPI	4',6-diamidino-2-phenylindole
DDC	diethyldithiocarbamate
ECM	extracellular matrix

FACS	fluorescence-activated cell sorting
FBS	fetal bovine serum
FPC	fibrocystin/polyductin
HSC	hepatic stellate cells
IL	interleukin
IP-10	interferon-γ-induced protein
K19	cytokeratin-19
KC	keratinocyte chemoattractant
LAP	latency associated peptide
MCP-1	monocyte chemotactic protein-1
MDR	multi-drug resistance
rsTGF-βRII-FC	recombinant soluble TGFβ receptor type II-FC fusion protein
TGFβ	transforming growth factor-β
TGFR	transforming growth factor receptor
TNFα	tumor necrosis factor-α
WT	wild type

REFERENCES

1. Ward CJ, Yuan D, Masyuk TV, Wang X, Punyashthiti R, Whelan S, et al. Cellular and subcellular localization of the ARPKD protein; fibrocystin is expressed on primary cilia. Hum Mol Genet. 2003; 12:2703–2710. [PubMed: 12925574]
2. Zhang MZ, Mai W, Li C, Cho SY, Hao C, Moeckel G, et al. PKHD1 protein encoded by the gene for autosomal recessive polycystic kidney disease associates with basal bodies and primary cilia in renal epithelial cells. Proc Natl Acad Sci U S A. 2004; 101:2311–2316. [PubMed: 14983006]
3. Lazaridis KN, Strazzabosco M, Larusso NF. The cholangiopathies: disorders of biliary epithelia. Gastroenterology. 2004; 127:1565–1577. [PubMed: 15521023]
4. Nakanuma Y, Harada K, Sato Y, Ikeda H. Recent progress in the etiopathogenesis of pediatric biliary disease, particularly Caroli's disease with congenital hepatic fibrosis and biliary atresia. Histol Histopathol. 2010; 25:223–235. [PubMed: 20017109]
5. Spirli C, Locatelli L, Morell CM, Fiorotto R, Morton SD, Cadamuro M, et al. PKA dependent p-Ser^{675}β-catenin, a novel signaling defect in a mouse model of Congenital Hepatic Fibrosis. Hepatology. 2013; 58:1713–1723. [PubMed: 23744610]
6. Anson M, Crain-Denoyelle AM, Baud V, Chereau F, Gougelet A, Terris B, et al. Oncogenic beta-catenin triggers an inflammatory response that determines the aggressiveness of hepatocellular carcinoma in mice. J Clin Invest. 2012; 122:586–599. [PubMed: 22251704]
7. Medzhitov R. Origin and physiological roles of inflammation. Nature. 2008; 454:428–435. [PubMed: 18650913]
8. Nichols MT, Gidey E, Matzakos T, Dahl R, Stiegmann G, Shah RJ, et al. Secretion of cytokines and growth factors into autosomal dominant polycystic kidney disease liver cyst fluid. Hepatology. 2004; 40:836–846. [PubMed: 15382115]

9. Fabris L, Cadamuro M, Fiorotto R, Roskams T, Spirlí C, Melero S, et al. Effects of angiogenic factor overexpression by human and rodent cholangiocytes in polycystic liver diseases. Hepatology. 2006; 43:1001–1012. [PubMed: 16628643]
10. Gallagher AR, Esquivel EL, Briere TS, Tian X, Mitobe M, Menezes LF, et al. Biliary and pancreatic dysgenesis in mice harboring a mutation in *Pkhd1*. Am J Pathol. 2008; 172:417–429. [PubMed: 18202188]
11. de Meijer VE, Sverdlov DY, Popov Y, Le HD, Meisel JA, Nosé V, et al. Broad-spectrum matrix metalloproteinase inhibition curbs inflammation and liver injury but aggravates experimental liver fibrosis in mice. PLoS One. 2010; 5:e11256. [PubMed: 20593020]
12. Sato A, Nakashima H, Nakashima M, Ikarashi M, Nishiyama K, Kinoshita M, et al. Involvement of the TNF and FasL produced by CD11b Kupffer cells/macrophages in CCl4-induced acute hepatic injury. PLoS One. 2014; 9:e92515. [PubMed: 24667392]
13. Popov Y, Patsenker E, Fickert P, Trauner M, Schuppan D. Mdr2 (*Abcb4*)−/− mice spontaneously develop severe biliary fibrosis via massive dysregulation of pro- and antifibrogenic genes. J Hepatol. 2005; 43:1045–1054. [PubMed: 16223543]
14. Popov Y, Patsenker E, Stickel F, Zaks J, Bhaskar KR, Niedobitek G, et al. Integrin αVβ6 is a marker of the progression of biliary and portal liver fibrosis and a novel target for antifibrotic therapies. J Hepatol. 2008; 48:453–464. [PubMed: 18221819]
15. Teicher BA, Fricker SP. CXCL12 (SDF-1)/CXCR4 pathway in cancer. Clin Cancer Res. 2010; 16:2927–2931. [PubMed: 20484021]
16. Patsenker E, Popov Y, Stickel F, Jonczyk A, Goodman SL, Schuppan D. Inhibition of integrin αVβ6 on cholangiocytes blocks TGF-β activation and retards biliary fibrosis progression. Gastroenterology. 2008; 135:660–670. [PubMed: 18538673]
17. O'Brien K, Font-Montgomery E, Lukose L, Bryant J, Piwnica-Worms K, Edwards H, et al. Congenital hepatic fibrosis and portal hypertension in autosomal dominant polycystic kidney disease. J Pediatr Gastroenterol Nutr. 2012; 54:83–89. [PubMed: 21694639]
18. Dranoff JA, Wells RG. Portal fibroblasts: Underappreciated mediators of biliary fibrosis. Hepatology. 2010; 51:1438–1444. [PubMed: 20209607]
19. Fausther M, Lavoie EG, Dranoff JA. Contribution of Myofibroblasts of Different Origins to Liver Fibrosis. Curr Pathobiol Rep. 2013; 1:225–230. [PubMed: 23997993]
20. Antoniades CG, Quaglia A, Taams LS, Mitry RR, Hussain M, Abeles R, et al. Source and characterization of hepatic macrophages in acetaminophen-induced acute liver failure in humans. Hepatology. 2012; 56:735–746. [PubMed: 22334567]
21. Sica A, Invernizzi P, Mantovani A. Macrophage plasticity and polarization in liver homeostasis and pathology. Hepatology. 2014; 59:2034–2042. [PubMed: 24115204]
22. Sica A, Mantovani A. Macrophage plasticity and polarization: in vivo veritas. J Clin Invest. 2012; 122:787–795. [PubMed: 22378047]
23. Morland CM, Fear J, McNab G, Joplin R, Adams DH. Promotion of leukocyte transendothelial cell migration by chemokines derived from human biliary epithelial cells in vitro. Proc Assoc Am Physicians. 1997; 109:372–382. [PubMed: 9220535]
24. Hsieh CS, Huang CC, Wu JJ, Chaung HC, Wu CL, Chang NK, et al. Ascending cholangitis provokes IL-8 and MCP-1 expression and promotes inflammatory cell infiltration in the cholestatic rat liver. J Pediatr Surg. 2001; 36:1623–1628. [PubMed: 11685687]
25. Lamireau T, Zoltowska M, Levy E, Yousef I, Rosenbaum J, Tuchweber B, et al. Effects of bile acids on biliary epithelial cells: proliferation, cytotoxicity, and cytokine secretion. Life Sci. 2003; 72:1401–1411. [PubMed: 12527037]
26. Munger JS, Huang X, Kawakatsu H, Griffiths MJ, Dalton SL, Wu J, et al. The integrin αVβ6 binds and activates latent TGF-β1: a mechanism for regulating pulmonary inflammation and fibrosis. Cell. 1999; 96:319–328. [PubMed: 10025398]
27. Duffield JS, Forbes SJ, Constandinou CM, Clay S, Partolina M, Vuthoori S, et al. Selective depletion of macrophages reveals distinct, opposing roles during liver injury and repair. J Clin Invest. 2005; 115:56–65. [PubMed: 15630444]
28. Wynn TA, Chawla A, Pollard JW. Macrophage biology in development, homeostasis and disease. Nature. 2013; 496:445–455. [PubMed: 23619691]

29. Vieira SM, Lemos HP, Grespan R, Napimoga MH, Dal-Secco D, Freitas A, et al. A crucial role for TNF-alpha in mediating neutrophil influx induced by endogenously generated or exogenous chemokines, KC/CXCL1 and LIX/CXCL5. Br J Pharmacol. 2009; 158:779–789. [PubMed: 19702783]

30. Fabris L, Strazzabosco M. Epithelial-mesenchymal interactions in biliary diseases. Semin Liver Dis. 2011; 31:11–32. [PubMed: 21344348]

31. Milani S, Herbst H, Schuppan D, Hahn EG, Stein H. In situ hybridization for procollagen types I, III and IV mRNA in normal and fibrotic rat liver: evidence for predominant expression in nonparenchymal liver cells. Hepatology. 1989; 10:84–92. [PubMed: 2737606]

32. Milani S, Herbst H, Schuppan D, Riecken EO, Stein H. Cellular localization of laminin gene transcripts in normal and fibrotic human liver. Am J Pathol. 1989; 134:1175–1182. [PubMed: 2474253]

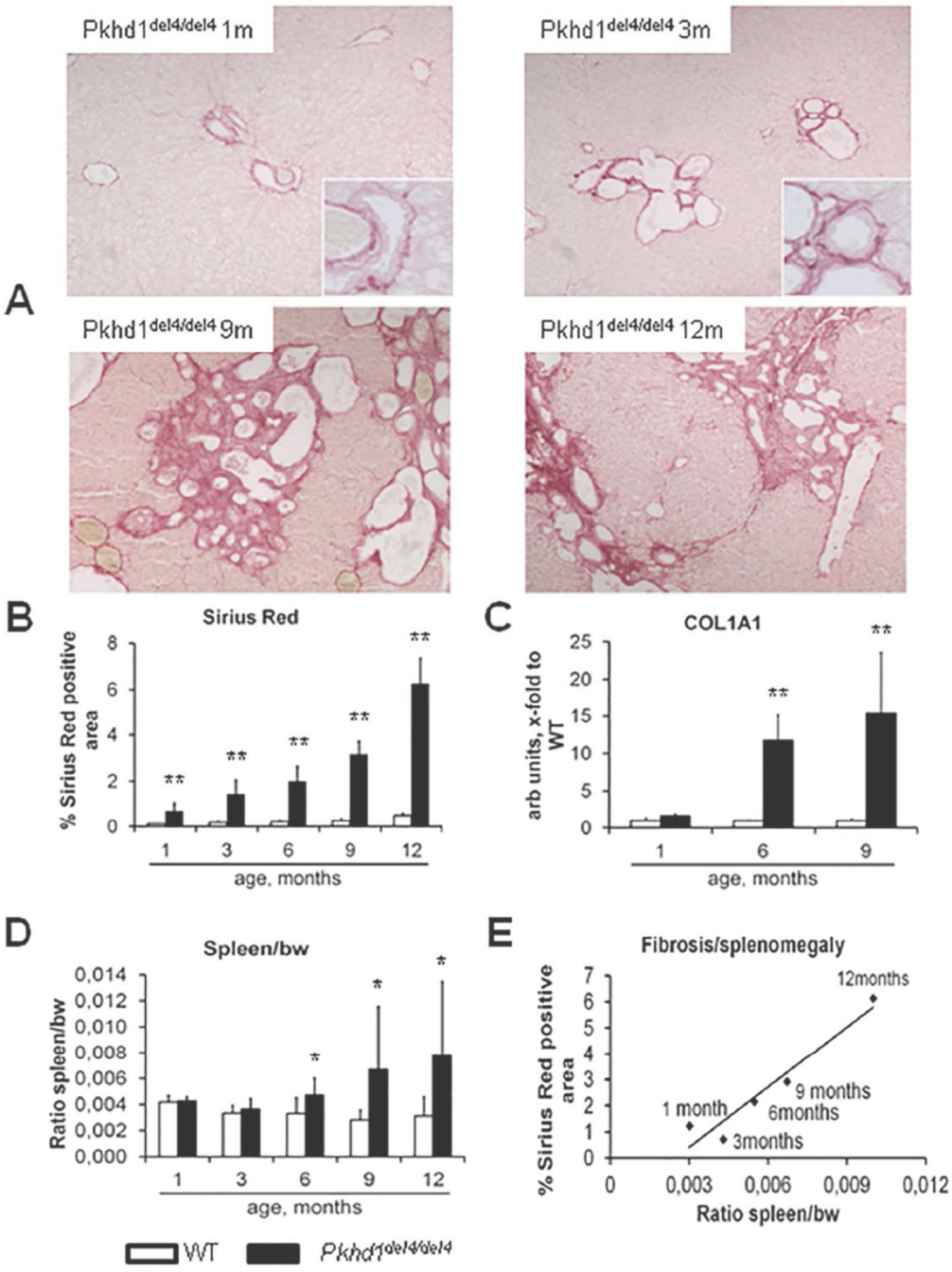

Figure 1. Age-dependent increase in peribiliary fibrosis correlates with portal hypertension in *Pkhd1*$^{del4/del4}$ mice

A. Micrographs of Sirius red stained liver sections taken from WT and *Pkhd1*$^{del4/del4}$ mice of different ages and indicating that peribiliary fibrosis develops progressively, starting at the pericystic region, and then extends through the portal area, finally leading to porto-portal septa formation (Sirius Red, M=100×). **B.** Morphometrical analysis of Sirius Red stained *Pkhd1*$^{del4/del4}$ mouse livers trough maturation (% are covered by Sirius red, n=from 4 to 7 for each age). **C.** Similarly, gene expression of COL1(A1) in whole liver lysates increased

slowly, reaching a 15-fold increase at 9 months (n=3 for each age). **D**. Splenomegaly (measured as the spleen weight/body weight) a surrogate markers of portal hypertension in CHF, became significant at 6 months, and increased thereafter (n=4/7 for each age). **E**. The extent of portal fibrosis (Sirius red) strongly and positively correlated with splenomegaly ($r=0.96$, $p<0.01$). *$p<0.05$ vs WT (same age), **$p<0.01$ vs WT (same age).

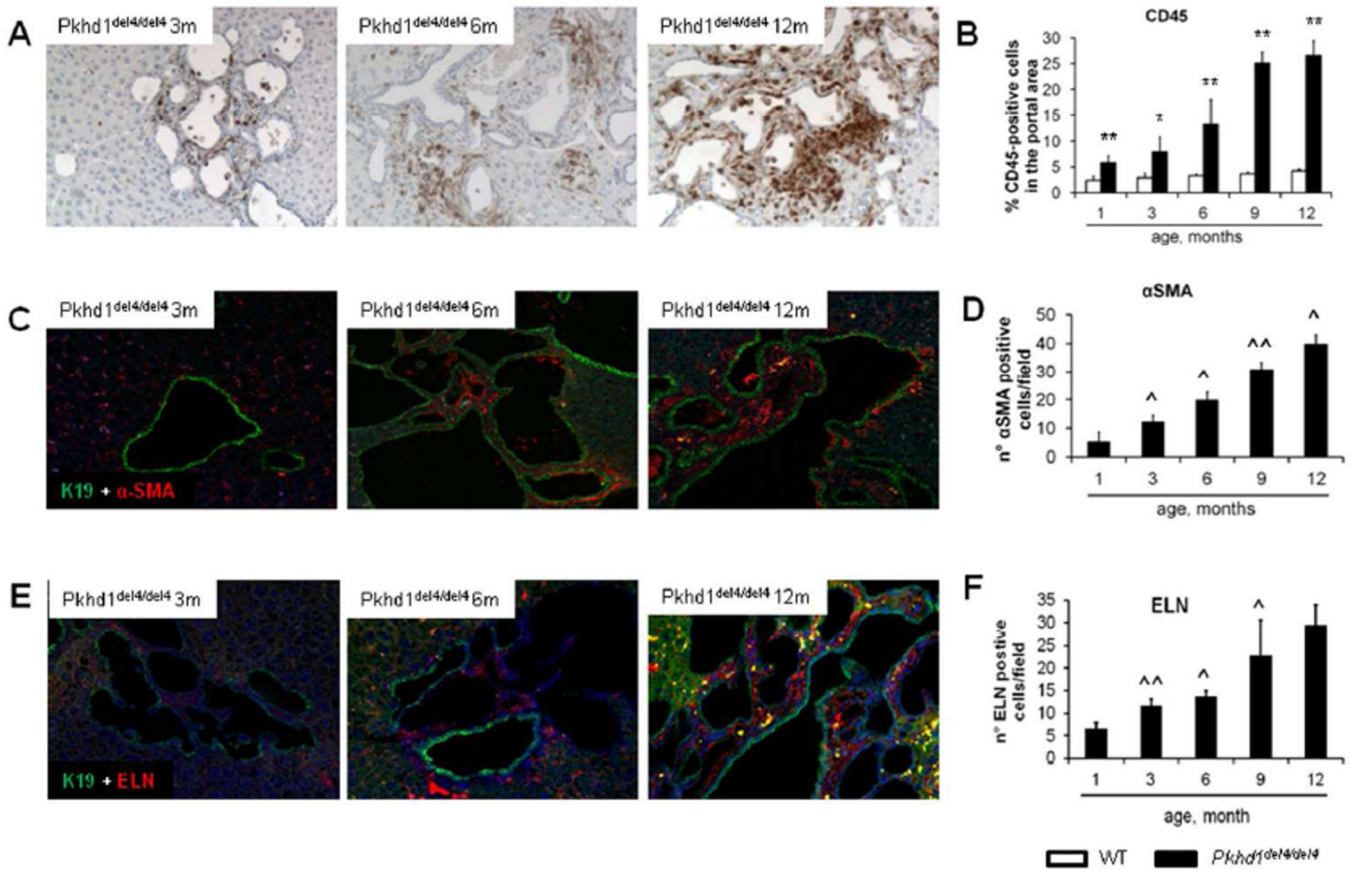

Figure 2. The progressive peribiliary accumulation of inflammatory cells in the portal tract, co-expressing F4/80 (macrophage marker) contrasts with the initial scarce contribution of myofibroblasts

A. A progressive portal accumulation of $CD45^+$ inflammatory cells adjacent to biliary cysts was observed (immunoperoxidase for CD45, M=200×). **B**. Amount of $CD45^+$ cells was quantified by morphometric analysis (n=3 for each age). **C.** In *Pkhd1*$^{del4/del4}$ mice, α-SMA^+ myofibroblasts scattered within the portal space (dual immunofluorescence for α-SMA - in red, and K19 - in green, M=200×). **D.** The number increased slowly through maturation with a linear pattern (n=3 for each age). **E**. Similarly to α-SMA, elastin $(ELN)^+$ portal fibroblasts accumulated into the portal space in a timedependent fashion (dual immunofluorescence for ELN - in red, and K19 - in green, M=200×). **F.** As quantified by morphometry, the number of ELN^+ cells augmented through maturation, with the most relevant increase after 6 months (n=4 for each age). *p<0.05 vs WT (same age), **p<0.01 vs WT (same age); ^p<0.05 vs previous maturation age, ^^p<0.01 vs previous maturation age.

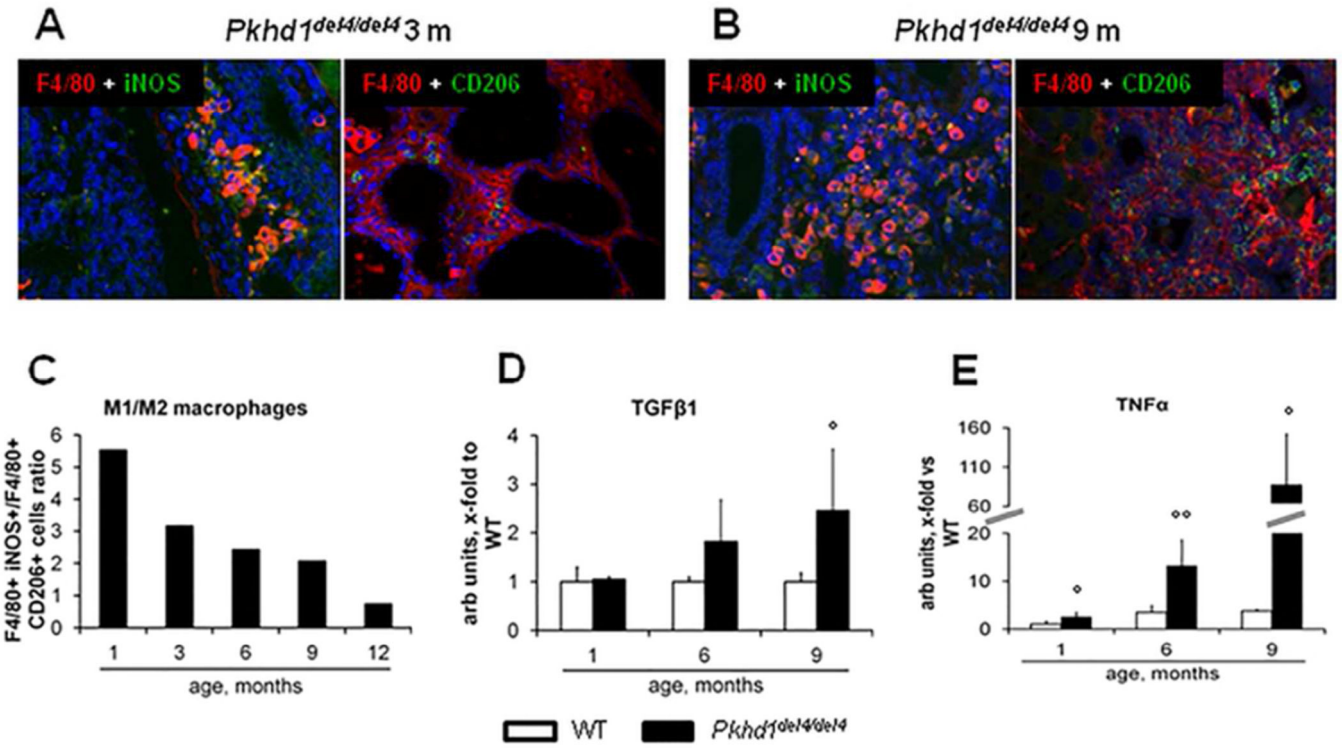

Figure 3. The initial M1 macrophage infiltrate is then matched by M2 cells

A–B. By dual immunofluorescence with the macrophage marker F4/80 (red), we evaluated the relative proportion of the macrophage phenotypes in the portal infiltrate, M1 (iNOS$^+$, green) and M2 (CD206$^+$, green), through the different ages (A, representative sample, 3 months; B, representative sample, 9 months, M=200×). **C.** Until the 9th month, the macrophage population was dominated by the M1 phenotype, but the relative proportion of M2 macrophages increased progressively, reaching that of M1 at the 12th month, as shown by the changes in the M1/M2 ratio through maturation (n=3 for each age). **D**. Consistent with this temporal sequence, gene expression of TGFβ1 (an M2 cytokine) in the whole liver increased mildly in the first phase, becoming significant only at 9 months (2.5-folds with respect to WT) (n=3 for each age). **E.** Up-regulation of TNFα (an M1 cytokine) was instead evident since the early stage of the disease, reaching 80-fold expression with respect to WT livers at 9 months (n=3 for each age). °p<0.05 vs WT (1 month), °°p<0.01 vs WT (1 month).

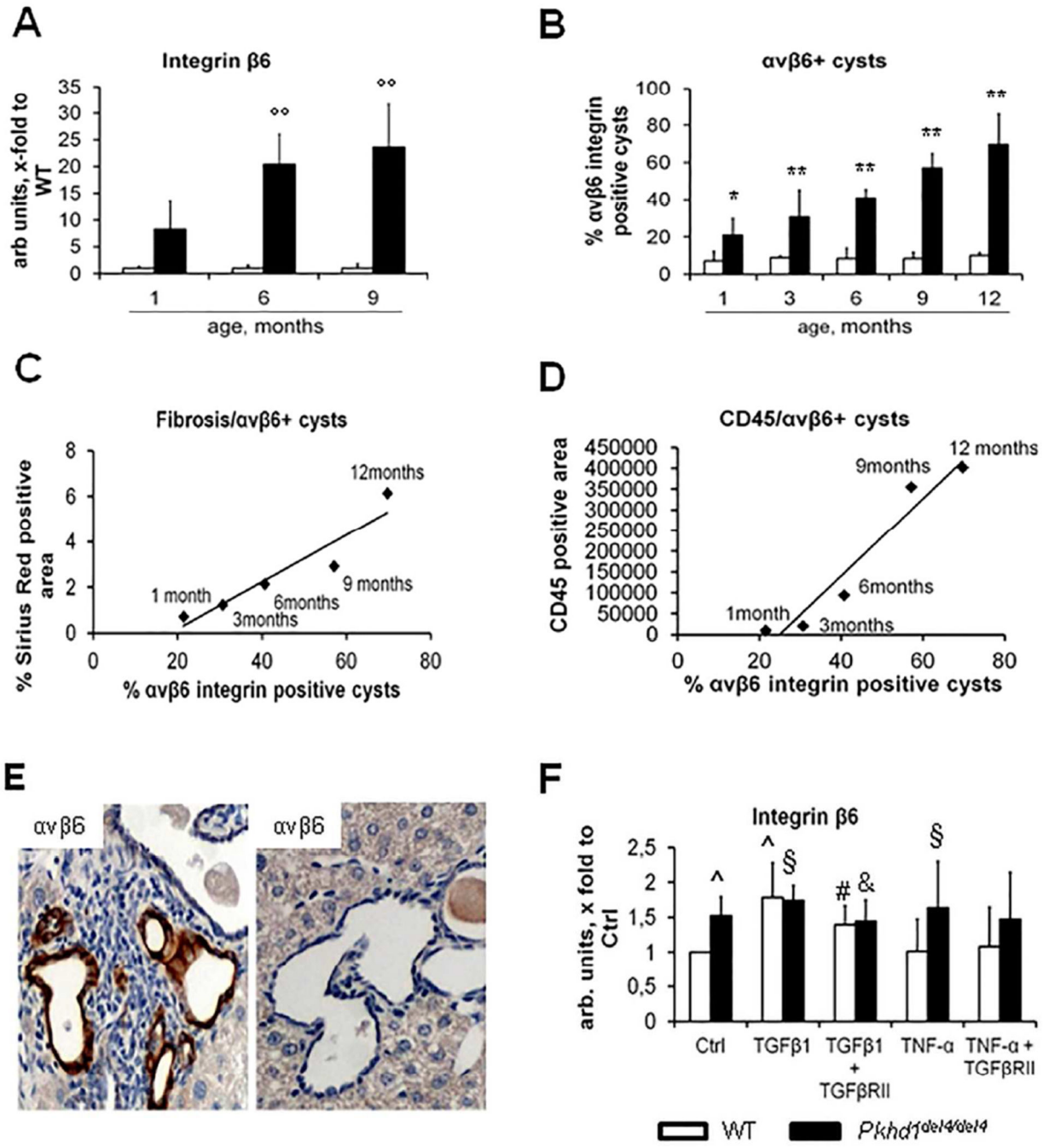

Figure 4. αvβ6 integrin expression correlates with portal fibrosis and peribiliary accumulation of CD45$^+$ cells in *Pkhd1*$^{del4/del4}$ mice

A. In contrast with WT mice, *Pkhd1*$^{del4/del4}$ mice showed a progressive increase in β6 gene expression in whole liver, which was greater than 25-fold at 6 months and nearly 35-fold at 9 months (n=3 for each age). **B.** Similarly, αvβ6 integrin expression on cyst epithelia assessed by immunohistochemistry increased progressively, reaching nearly the 70% of biliary structures at 12 months (n=3/5 for each age). **C–D**. Immunohistochemical expression of αvβ6 strongly correlated both with portal fibrosis (r=0.94, p<0.02) and with the CD45$^+$

portal cell infiltrate (r=0.97, p<0.01). **E.** In any given specimen, αvβ6 integrin was typically higher in biliary cysts surrounded by a dense inflammatory infiltrate (immunoperoxidase for αvβ6, representative sample, 6 months, M= 400×). **F**. TGFβ1 and TNFα stimulate gene expression of β6 integrin in *Pkhd1*$^{del4/del4}$ cholangiocytes. In *Pkhd1*$^{del4/del4}$ cholangiocytes, β6 mRNA was significantly increased in basal conditions with respect to WT. In both WT and *Pkhd1*$^{del4/del4}$ cholangiocytes, β6 expression was further and significantly increased after TGFβ1. Unlike TGFβ1, TNFα significantly increased β6 mRNA expression only in *Pkhd1*$^{del4/del4}$ cholangiocytes. TGFβRII blockade abolished the TGFβ1 effects on β6 mRNA expression in both *Pkhd1*$^{del4/del4}$ and WT cholangiocytes, in contrast to TNFα whose effects on β6 were unaffected by TGFβRII antagonism (n=6/10 for each experimental condition, cultured cholangiocytes derived from mice of 3 months of age). °°p<0.01 vs WT (1 month), *p<0.05 vs WT (same age), **p<0.01 vs WT (same age), ^p<0.05 vs WT Ctrl, §p<0.05 vs *Pkhd1*$^{del4/del4}$ Ctrl, $^{\#}$p<0.05 vs WT TGFβ1-treated, $^{\&}$p<0.05 vs *Pkhd1*$^{del4/del4}$ TGFβ1-treated.

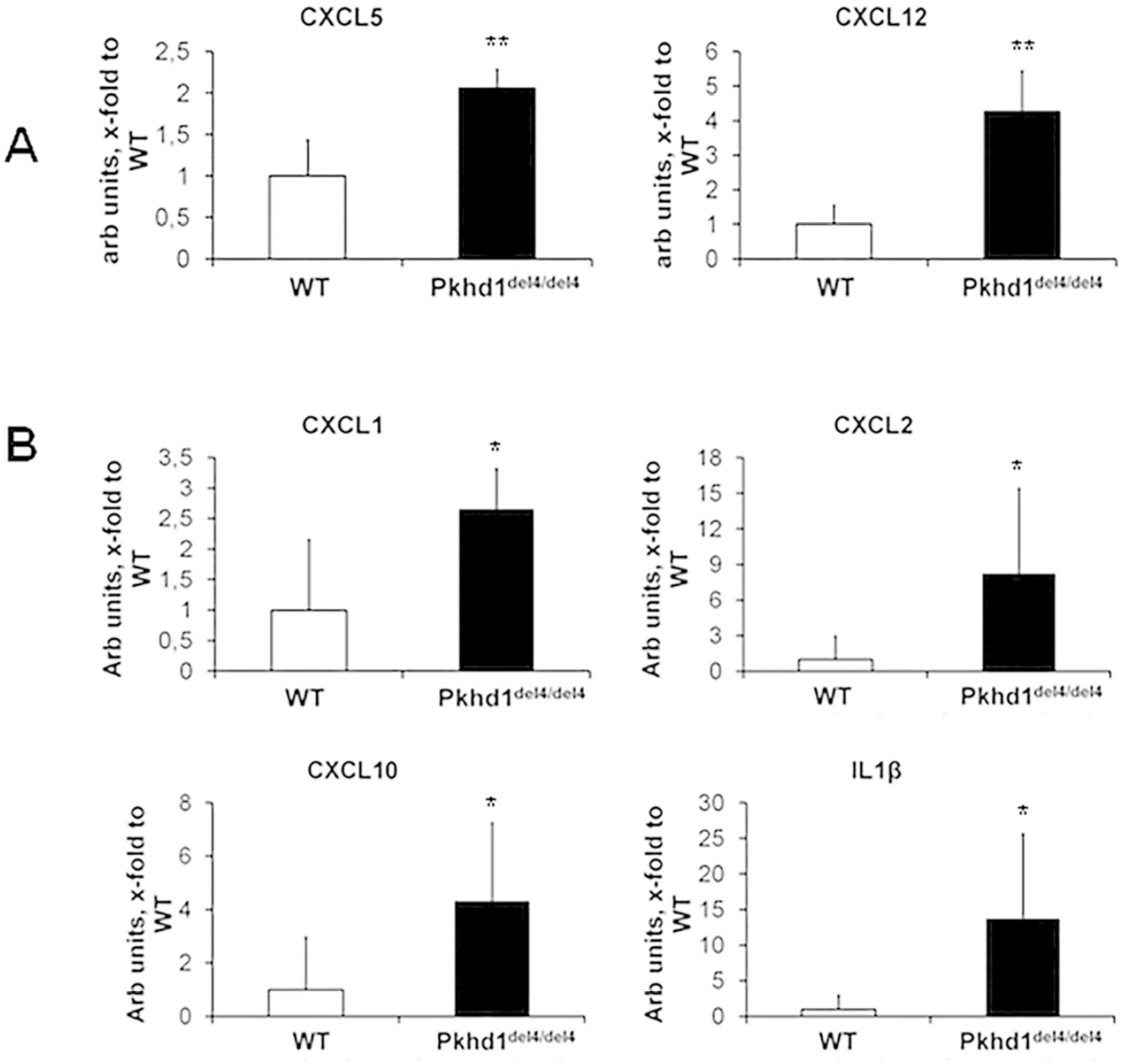

Figure 5. Gene expression analysis of biliary K19 positive structures isolated from *Pkhd1*$^{del4/del4}$ and WT mice by LCM shows an increase in CXCL5, CXCL12, CXCL1, CXCL2, CXCL10 and IL1β

To identify the soluble factors mediating macrophage recruitment by *Pkhd1*$^{del4/del4}$ cholangiocytes, gene expression of a number of cytokines previously shown to be secreted by cholangiocytes in culture, was assessed in mRNA selectively captured from epithelial cells lining biliary cysts of *Pkhd1*$^{del4/del4}$ and normal ducts of WT mice at 1 and 3 months of age by LCM. **A**. LIX/CXCL5 and SDF1/CXCL12 were already significantly increased in biliary cysts of *Pkhd1*$^{del4/del4}$ mice at 1 month. **B.** Also KC/CXCL1, MIP-2/CXCL2, IP- 10/ CXCL10, SDF1/CXCL12 and IL-1β became significantly increased at 3 months of age (n=4 for WT, n=5 for *Pkhd1*$^{del4/del4}$ for both ages). *p<0.05 vs WT, **p<0.01 vs WT.

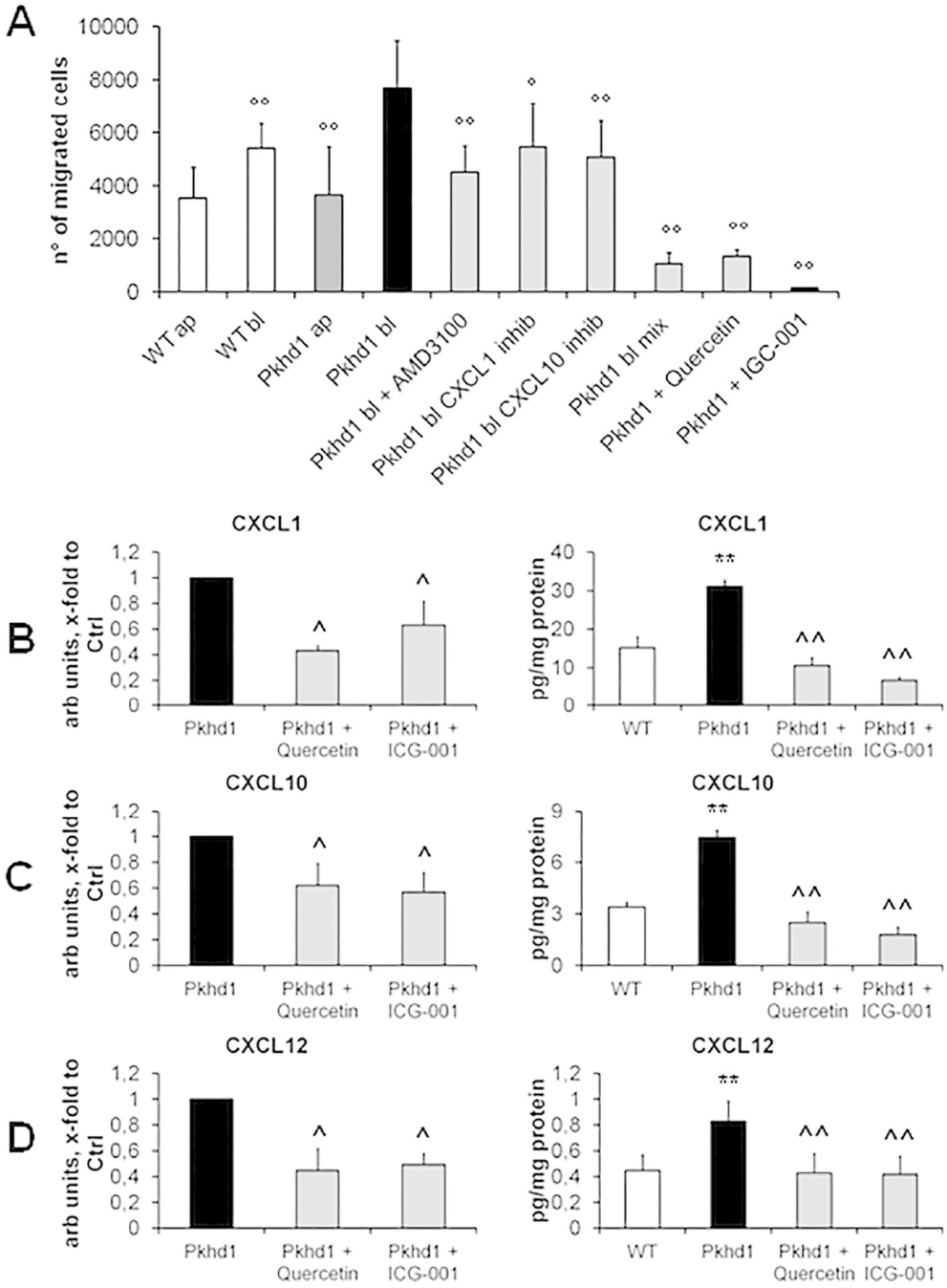

Figure 6. Basolateral conditioned medium of *Pkhd1*$^{del4/del4}$ cholangiocytes contains chemokines able to stimulate macrophage recruitment

A. Migration of RAW 264.7 macrophages was measured in Boyden chambers containing conditioned medium. In *Pkhd1*$^{del4/del4}$ cholangiocytes, basolateral conditioned medium (bl) induced a stronger migratory effect of RAW 264.7 macrophages than the apical medium, or the basolateral medium from WT cholangiocytes (n=4 for both experiments). This effect was significantly inhibited by specific antagonism of CXCL1, CXCL10 and CXC12, and abolished by combined antagonism of CXCL1+CXCL10+CXCL12 or by inhibition of β-

catenin signaling with quercetin (50 μM) or ICG-001 (25 μM) (n=4 for each experiment). **B–D**. As compared with WT, *Pkhd1*$^{del4/del4}$ cultured cholangiocytes expressed significantly higher amounts of CXCL1 (**B**), CXCL10 (**C**) and CXCL12 (**D**) both at mRNA (n=7 for each chemokine) and protein levels in the basolateral medium (n=3 for CXCL1 and CXCL10, n=12 for CXCL12); all chemokine expression levels were significantly reduced by inhibition of β-catenin signaling with quercetin (50 μM) or ICG-001 (25 μM) (n=7 for each chemokine for RT-PCR experiments, n=4 for each chemokine for ELISA experiments) (cholangiocytes derived from mice of 3 months of age). **p<0.01 vs WT, ^p<0.05 vs *Pkhd1*, ^^p<0.01 vs *Pkhd1*, °p<0.05 vs *Pkhd1* bl, °°p<0.01 vs *Pkhd1* bl.

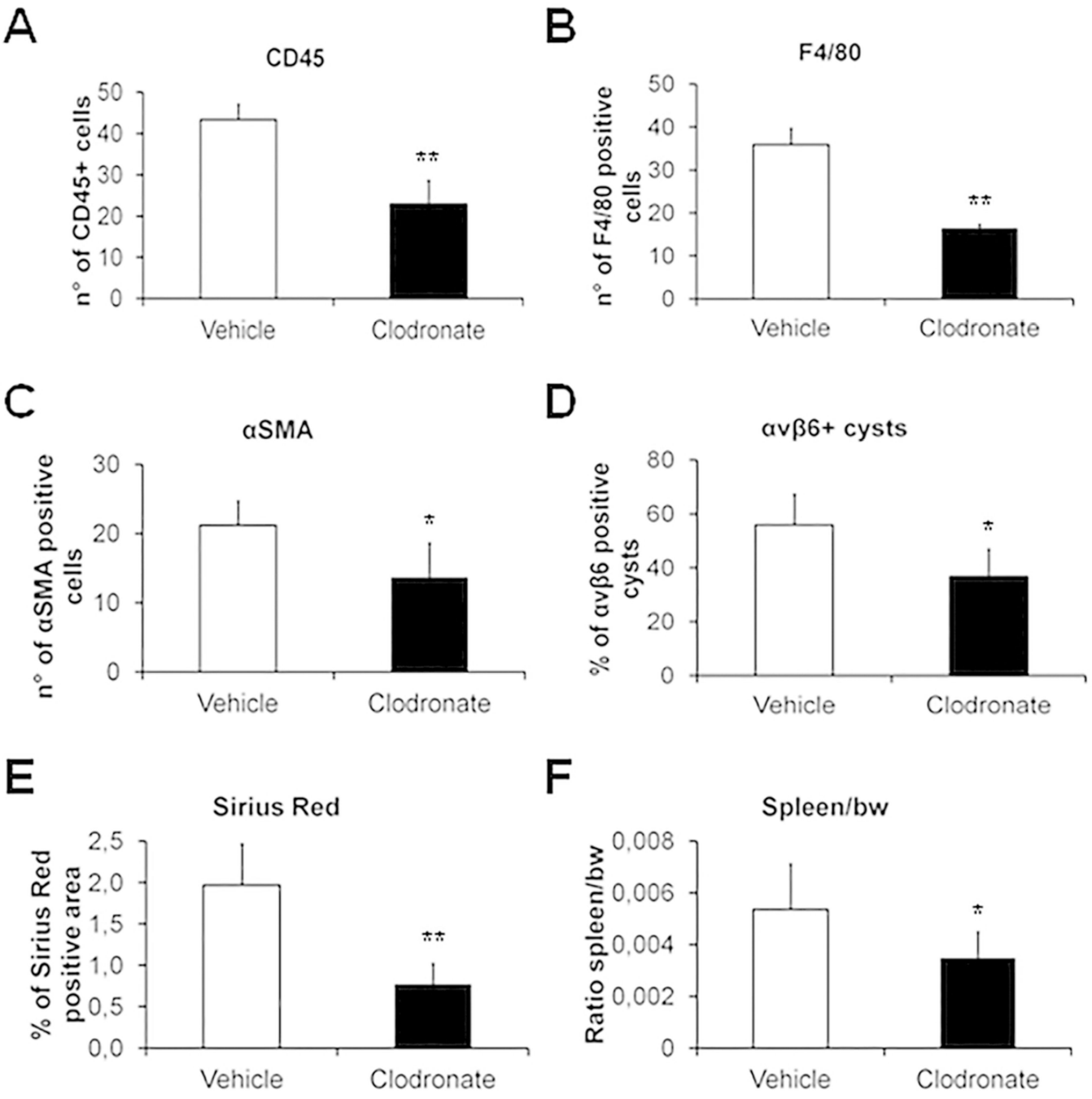

Figure 7. Macrophage depletion induced by clodronate halts fibrosis progression and development of portal hypertension and reduces αvβ6 integrin biliary expression, macrophage infiltration and myofibroblast activation in *Pkhd1*$^{del4/del4}$ mice

A–F. Clodronate treatment resulted in a significant reduction in the number of CD45^{+} (inflammatory cells, **A**), F4/80^{+} (macrophages, **B**) and α-SMA^{+} cells (myofibroblasts, **C**), as well as in the expression of αvβ6 on biliary structures (**D**), and in portal fibrosis (Sirius Red staining of the peribiliary area, **E**). Noteworthy, hampering peribiliary fibrosis at this stage is clinically relevant since it prevents development of portal hypertension, as shown by the significant reduction in splenomegaly (spleen/body weight, **F**) (n=3 vehicle, n= 4 clodronate

treated). Representative images of both experimental groups are given in Supplemental Figure 8. *p<0.05 vs vehicle, **p<0.01 vs vehicle.

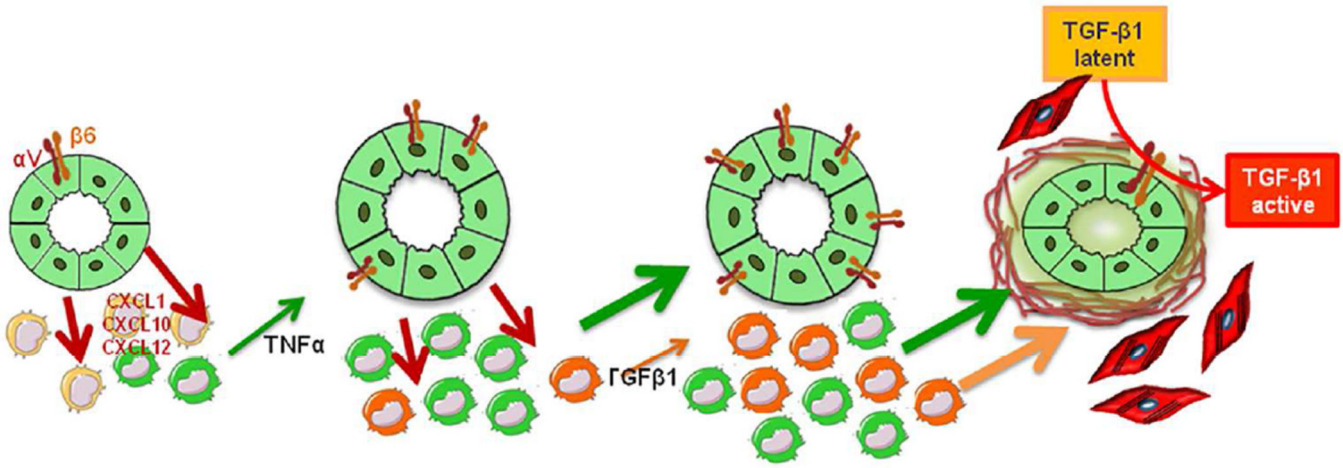

Figure 8. Working model: cross-talk between cholangiocytes and macrophages stimulates peribiliary fibrosis in *Pkhd1*$^{del4/del4}$ mice

In *Pkhd1*$^{del4/del4}$ mice, portal fibrosis is the result of an intensive cross-talk between epithelial and inflammatory cells, originating from the FPC-deficient cholangiocytes. By secreting a range of chemokines, including CXCL1, CXCL10 and CXCL12, likely secondary to β-catenin signaling over-activation, *Pkhd1*$^{del4/del4}$ cholangiocytes recruit macrophages in the portal area and stimulate their secretory functions. In the early phases, this portal infiltrate is mainly composed by M1 macrophages (green peribiliary cells), and TNFα (green arrow) is the predominant cytokine released until also TGFβ1 (orange arrow) becomes significantly secreted by M2 macrophages (orange peribiliary cells). Both macrophage-derived cytokines up-regulate αvβ6 integrin expression on biliary cysts and this, in turn, activates latent TGFβ1. Once activated, TGFβ1 induces production of collagen by cyst cholangiocytes, and as the disease progresses, by myofibroblasts, ultimately resulting in excessive matrix deposition into the peribiliary region.